International Journal of Thermal Sciences 49 (2010) 99–108

Contents lists available at ScienceDirect

International Journal of Thermal Sciences

journal homepage: www.elsevier.com/locate/ijts

A study of liquid flow in a flat plate heat pipe under localized heating

B.K. Tan [1], T.N. Wong*, K.T. Ooi

School of Mechanical and Aerospace Engineering, Nanyang Technological University, Nanyang Avenue, Singapore 639798, Singapore

ARTICLE INFO

Article history:
Received 10 July 2008
Received in revised form
2 January 2009
Accepted 12 June 2009
Available online 12 August 2009

Keywords:
Green's function
Heat pipe
Point source

ABSTRACT

An analytical approach is presented to study the liquid flow performances inside the wick structure of a flat plate heat pipe under different types of heat source conditions. Starting from a point heat source on the heat pipe, different types of heat sources such as line, strip and discrete heaters are simulated using the Green's function approach together with the respective source distribution functions. The corresponding liquid pressure and velocity distributions are illustrated and discussed. The work is then extended to simulate multiple discrete heat source condition on the heat pipe. This analytical model is validated with the available results in the literature and good agreement is obtained. The work presented is advantageous in the thermal management as this could help to determine the optimum heat source positions on the heat pipe, which will allow efficient cooling of the electronic components or system.

1. Introduction

Thermal management using flat plate heat pipes is an efficient way in the cooling and spreading of high heat flux electronic devices such as integrated circuits (IC) chips. Due to the growing trends of integrating and miniaturizing of electronic systems, more IC chips could be incorporated onto a single printed circuit board (PCB). Thus, this would inevitably generate more hot spots at the board level. Therefore, if a flat plate heat pipe were to be employed as the heat-dissipating medium, it would be advantageous to evaluate the heat pipe performance under multiple-source heating condition.

Since heat pipes have the ability to transport heat over a substantial distance at low temperature drops, it has made them a much reliable and efficient device for the heat-spreading requirement. The working liquid's circulation inside the wick structure of a flat plate heat pipe is very important because it influences directly the capillary limit of the cooling device [1]. This capillary limit, which is commonly known as the heat transport capacity, represents the total amount of heat that can be transferred before the occurrence of the 'dry-out' situation at the evaporator section. When this happens, the circulation inside the wick structure will stop and cause the temperature to increase at the evaporator section.

In the literature, both Vafai and Wang [2] had presented an analytical study for the vapor and liquid flow of an asymmetrical flat plate heat pipe. A pseudo three-dimensional flow field was bifurcated on the x–y plane due to the asymmetrical nature of the heat sources and sinks. In their work, the overall axial pressure distributions of both the vapor and liquid phases in the heat pipe were obtained. The results from this analytical model had provided good qualitative agreement when compared with those based on the solutions of the field equations for the conventional symmetrical case.

In addition, Huang and Liu [3] had reported an analytical model to calculate the distributions of the liquid pressure and velocity in the isotropic wick structure of a flat plate heat pipe. In their work, a two-dimensional heater was fixed at the end of the heat pipe under localized heating condition and their results revealed that the best position to place a heater is at the mid-section of the heat pipe.

For heat pipes with multiple heat sources, both Faghri and Buchko [4] had carried out experimental and numerical analysis for circular heat pipes operating at low temperatures. It was concluded that the maximum heat load on the heat pipe varied greatly with the locations of the local heat fluxes. In addition, an analytical study of a flat plate heat pipe under multiple point source heating condition was presented by Tan et al. [5]. In their work, point sources were modeled as the heat input to the device and various optimized heat source's positions were obtained based on the minimal liquid pressure drop across the wick structure of the device.

The liquid flow characteristics inside the wick structure of a flat plate heat pipe vary differently according to the various heating

* Corresponding author. Tel.: +65 790 5587; fax: +65 791 1859.
E-mail address: mtnwong@ntu.edu.sg (T.N. Wong).
[1] Now Manager - Strategic Plans, ST Engineering Ltd, 51 Cuppage Road, #09-08, Starhub Centre, Singapore 229469.

1290-0729/$ – see front matter © 2009 Elsevier Masson SAS. All rights reserved.
doi:10.1016/j.ijthermalsci.2009.06.013

Nomenclature

a	length of the flat plate heat pipe [m]
A_{mn}	fourier coefficients of p
b	width of the flat plate heat pipe [m]
$\delta(x-\zeta)\delta(x-\psi)$	an expression of a Delta function
$f(\zeta,\psi)$	a distribution function of a Poisson equation
$f(x,y)$	distribution function of the condensation rate
F_{mn}	fourier coefficients of $f(x,y)$
$G(x,y;\xi,\psi)$	Green's function in two-dimensional form.
m,n	Fourier terms
$\Delta P_{\max}$	least maximum liquid pressure drop across the wick structure
ΔP	pressure difference [Pa]
p	pressure [Pa]
P_{ref}	reference pressure [Pa]
P	normalized liquid pressure
x_1,y_1	x and y coordinates of the point heat source [m]
X,Y	non-dimensional axial and transverse coordinates
u,v	velocity components in the x and y direction [m s^{-1}]
U,V	non-dimensional velocity components in the x and y direction

Greek symbol

η	dimensional ratio between the condensation and evaporation rate of the heat pipe

Subscript

C	center coordinates of the discrete heater
D	discrete heater
L	line heater
P	point heater
R	boundary region
S	strip heater

conditions at the evaporator section. When there is a complete heating at the evaporator section, the liquid flow will be one-dimensional. However, when there is a multiple partial heating condition, the liquid flow will become two-dimensional instead. In this paper, various types of heating condition on the flat plate heat pipe will be presented to demonstrate the corresponding liquid flow characteristics inside the heat pipe. Using the Green's function approach, the analytical liquid pressure drop and velocity vectors can be obtained for the different types of heating conditions such as line, strip and discrete heaters on the heat pipe as shown in Fig. 1. These analytical solutions can be very useful especially for cooling multiple discrete heat sources on the PCB when heat pipe is designated to be the heat-dissipating medium.

2. Analytical formulation

The liquid pressure and velocity solutions presented by Tan et al. [5] using the point source approach are used as the foundations to further develop the analytical liquid flow solutions of the various heat source on the flat plate heat pipe. Analytically, the solutions formulated from the point source approach are in the form of a Green's function. Hence, through further development of these equations could then extend to form the solutions for a line, strip or discrete heater on the heat pipe with appropriate heat source boundary conditions.

Mathematically, the derivation using the Green's function of a problem is briefly described based on the formulations listed in the literature [6]. Consider the following equation,

$$Lu(x) = f(x) \tag{1a}$$

where L is a linear differential operator of a function $u(x)$ and $f(x)$ is a given function which is the source term of the problem while the solution is required on the interval of $0 \le x \le l$.

Instead of considering $f(x)$ as a continuous source function, an approximation of discrete source functions such that $f(\xi_1)$, $f(\xi_1)$, ……,$f(\xi_n)$ acting at the points $x = \xi_1$, $x = \xi_2$, ……., $x = \xi_n$, respectively, which all lie within the range of 0 $0 \le x \le l$. Thereafter, a function $G(x:\xi_k)$ can be defined to be solution of equation (1a) due to a unit point source acting at ξ_k, hence, by replacing $f(x)$ with $\delta(x\text{-}\xi k)$, the solution due the single effect is therefore $G(x:\xi_k)\ f(\xi_k)$. Thus, summing all such solutions for the entire n-points source terms acting on $0 \le x \le l$, the solution will take the form of:

$$u(x) = \sum_{k=1}^{n} G(x:\zeta_k) f(\zeta_k) \tag{1b}$$

As n terms become larger such that the number of point source functions $f(\xi n)$ increases and therefore a better approximation to

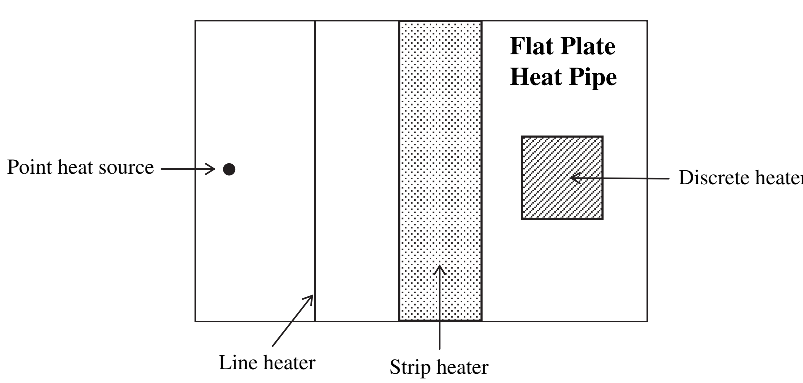

Fig. 1. The various types of heat sources on the flat plate heat pipe.

$f(x)$ can be obtained when $n \to \infty$, so as $\xi_k \to \xi_{k+1}$ for all k values. Thus, the summation of Equation (1b) will be replaced by an integral to give a required solution of equation (1a), which takes the form of:

$$u(x) = \int_0^l G(x:\zeta_k) f(\zeta_k) d\zeta \tag{1c}$$

where the function $G(x:\xi)$ is known as the Green's function of the problem.

Similarly, for the case of a two-dimensional Possion equation,

$$\nabla^2 u = f(x,y) \tag{2a}$$

the solution for the range of $0 \le x \le a,\ \ 0 \le y \le b$ is as follows:

$$u(x,y) = \int_0^a \int_0^b G(x,y;\zeta,\psi) f(\zeta,\psi) d\zeta d\psi \tag{2b}$$

where $G(x,y;\xi,\psi)$ will be the Green's function of this two-dimensional case, such that,

$$\nabla^2 G(x,y;\zeta,\psi) = \delta(x-\zeta)\delta(y-\psi) \tag{2c}$$

with $\delta(x-\zeta)\delta(x-\psi)$ being an expression of Delta function and$f(\zeta,\psi)$ is a distribution function of the Poisson equation. Thus, if the distribution function is known, the solution to the distribution function of the Poisson equation can therefore be determined. Thus, the formulations to form the Green function approach are developed.

The analytical liquid flow solutions in this paper are formulated from the solutions presented from [5] where the liquid flow model employing the point source approach is formulated using the mass conservation principle with the Darcy's liquid flow equations. The parameters used for non-dimensionalizing the pressure and velocities of the liquid flow model formulated in [5] are expressed as :

$$P = \frac{p - p_{ref}}{\beta ab} \tag{3a}$$

$$U = \frac{u}{\alpha^+ b/\rho} \tag{3b}$$

$$V = \frac{v}{\alpha^+ b/\rho} \tag{3c}$$

where α^+ is the condensation rate of the wick structure, β is the liquid condensation relationship within the wick structure having the expression of $(\mu\alpha^+/\rho K)$ such that μ is the dynamic viscosity of liquid, ρ is the liquid density and K is the wick permeability. a and b here refer to the length and width of the heat pipe respectively.

It is realized that the solutions from [5] are in the form of a Green's function, where the normalized liquid pressure P and velocity fields (U,V) inside the wick structure of the heat pipe can be expressed as follows:

$$P = P_{m0} + P_{0n} + P_{mn} = \sum_{m=1}^{\infty} A_{m0}\cos(m\pi X) + \sum_{n=1}^{\infty} A_{0n}\cos(n\pi Y) + \sum_{m=1}^{\infty}\sum_{n=1}^{\infty} A_{mn}\cos(m\pi X)\cos(n\pi Y) \tag{3d}$$

$$U = -\frac{\partial P}{\partial X} = U_{m0} + U_{mn} = \sum_{m=1}^{\infty} A_{m0}(m\pi)\sin(m\pi X) + \sum_{m=1}^{\infty}\sum_{n=1}^{\infty} A_{mn}(m\pi)\sin(m\pi X)\cos(n\pi Y) \tag{3e}$$

$$V = -\frac{a}{b}\frac{\partial P}{\partial X} = (V_{0n} + V_{mn}) = \frac{a}{b}\left\{ \sum_{n=1}^{\infty} A_{0n}(n\pi)\sin(n\pi Y) + \sum_{m=1}^{\infty}\sum_{n=1}^{\infty} A_{mn}(n\pi)\cos(m\pi X)\sin(n\pi Y) \right\} \tag{3f}$$

where the corresponding Fourier coefficients are represented as follows:

$$A_{m0} = \frac{2}{b^2(m\pi)^2} F_{m0} = \frac{-2a}{b(m\pi)^2}\cos\frac{m\pi x_1}{a} \tag{4a}$$

$$A_{0n} = \frac{2}{a^2(n\pi)^2} F_{0n} = \frac{-2b}{a(n\pi)^2}\cos\frac{n\pi y_1}{b} \tag{4b}$$

$$A_{mn} = \frac{4}{b^2(m\pi)^2 + a^2(n\pi)^2} F_{mn} = \frac{-4ab}{b^2(m\pi)^2 + a^2(n\pi)^2}\cos\frac{m\pi x_1}{a}\cos\frac{n\pi y_1}{b} \tag{4c}$$

In this paper, the liquid pressure and velocity fields in the wick structure of the heat pipe are evaluated analytically by considering the working fluid to be flowing in an isotropic wick structure with constant transport properties. The flow is also assumed to be steady, laminar and subsonic. In addition, symmetrical heating on the upper and lower heat pipe surfaces is considered. Thus, there will be two identical and independent liquid flows in the upper and lower wick structure of the heat pipe respectively. Hence, the analytical solutions are simplified to consider only the heat source on the upper surface of the heat pipe where the heat pipe is oriented horizontally.

2.1. Line heater

The pressure and velocity solutions of the liquid flow in the wick structure from the line heater can be obtained from equation (3). The analytical liquid pressure from the point source approach by Tan et al. [5] is shown below which is in the form of a Green's function, such that:

$$P(x,y)_{\mathrm{P}} = G(x,y|x_1,y_1) \tag{5}$$

with x_1 and y_1 being the coordinates of the point heat source on the heat pipe as shown in Fig. 2(a).

Since the corresponding liquid velocity expressions are related to the liquid pressure solution, therefore the liquid velocities could be written as,

$$U(x,y)_{\mathrm{P}} = -\frac{\partial P(x,y)_{\mathrm{P}}}{\partial x} \tag{6a}$$

$$V(x,y)_{\mathrm{P}} = -\frac{\partial P(x,y)_{\mathrm{P}}}{\partial y} \tag{6b}$$

where $U(x,y)_{\mathrm{P}}$ and $V(x,y)_{\mathrm{P}}$ are the velocities in the x and y direction respectively on the heat pipe.

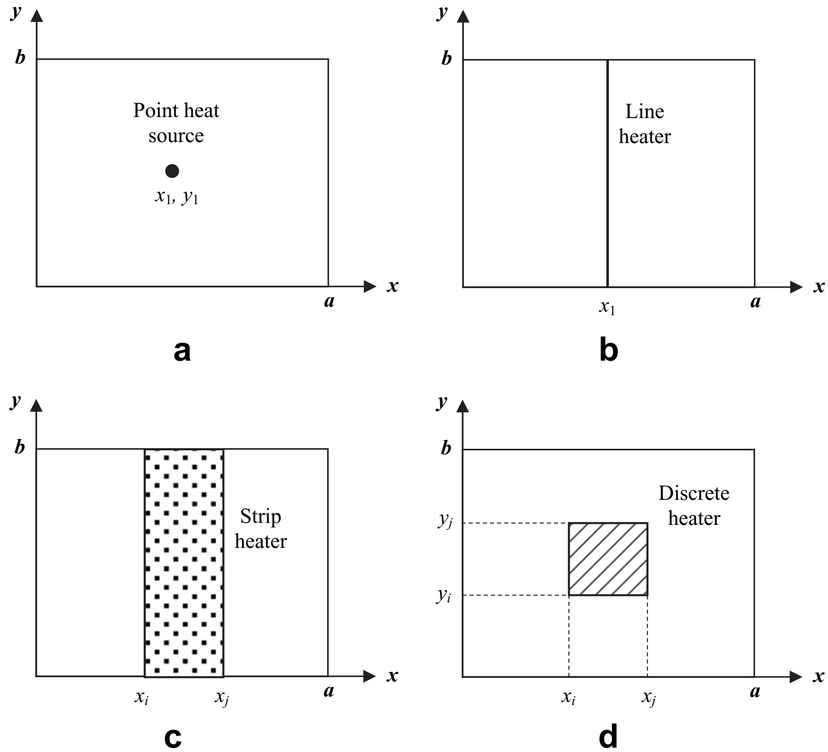

Fig. 2. Geometrical definitions of the various heat sources on the flat plate heat pipe: (a) point heat source, (b) line heater, (c) strip heater, and (d) discrete heater.

The liquid pressure solution per unit strength for the line heater can be obtained by integrating equation (5) together with the source distribution function of the line heater, such that,

$$P(x,y)_{\mathrm{L}} = \left(\frac{1}{-\eta_{\mathrm{P}}}\right) \iint\limits_{\mathrm{R}} f(x,y)_{\mathrm{L}} G(x,y|x_1,y_1)\mathrm{d}x_1\mathrm{d}y_1 \quad (7)$$

The velocity distributions for the line heater can then be obtained by considering equations (6a), (6b) and (7) respectively. Together, these are evaluated to be,

$$U(x,y)_{\mathrm{L}} = \frac{\partial}{\partial x}\left\{\left(\frac{1}{-\eta_{\mathrm{P}}}\right) \iint\limits_{\mathrm{R}} f(x,y)_{\mathrm{L}} G(x,y|x_1,y_1)\mathrm{d}x_1\mathrm{d}y_1\right\} \quad (8a)$$

$$V(x,y)_{\mathrm{L}} = \frac{\partial}{\partial y}\left\{\left(\frac{1}{-\eta_{\mathrm{P}}}\right) \iint\limits_{\mathrm{R}} f(x,y)_{\mathrm{L}} G(x,y|x_1,y_1)\mathrm{d}x_1\mathrm{d}y_1\right\} \quad (8b)$$

From Fig. 2(b), consider a line heater that extends entirely along the y direction $(0 \le y \le b)$ on the heat pipe with the following source distribution function:

$$f(x,y)_{\mathrm{L}} = 1 - \eta_{\mathrm{L}}\delta(x - x_1) \quad (9)$$

where η is defined as the dimensional ratio between the condensation and evaporation rate of the heat pipe.

Hence, using the Green's function application with $\eta_{\mathrm{L}} = a$, the formulation is then reduced to be one-dimensional and the liquid pressure solution for this line heater per unit strength is simplified to be:

$$P(x,y)_{\mathrm{L}} = \sum_{m=1}^{\infty}(A_{m0})_{\mathrm{L}}\cos(m\pi X) + \sum_{n=1}^{\infty}(A_{0n})_{\mathrm{L}}\cos(m\pi Y) + \sum_{m=1}^{\infty} \times \sum_{n=1}^{\infty}(A_{mn})_{\mathrm{L}}\cos(m\pi X)\cos(n\pi Y) \quad (10)$$

where the simplified Fourier coefficients $(A_{m0})_{\mathrm{L}}$, $(A_{0n})_{\mathrm{L}}$ and $(A_{mn})_{\mathrm{L}}$ are found to be:

$$(A_{m0})_{\mathrm{L}} = \frac{-2\eta_{\mathrm{L}}}{b(m\pi)^2}\cos\frac{m\pi x_1}{a} \quad (11a)$$

$$(A_{0n})_{\mathrm{L}} = 0 \quad (11b)$$

$$(A_{mn})_{\mathrm{L}} = 0 \quad (11c)$$

Subsequently, using equations (8a) and (8b), the following liquid velocity distributions for the line heater on the heat pipe are determined to be:

$$U(x,y)_{\mathrm{L}} = \sum_{m=1}^{\infty}(A_{m0})_{\mathrm{L}}(m\pi)\sin(m\pi X) + \sum_{m-1}^{\infty} \times \sum_{n=1}^{\infty}(A_{mn})_{\mathrm{L}}(m\pi)\sin(m\pi X)\cos(n\pi Y) \quad (12a)$$

$$V(x,y)_{\mathrm{L}} = \frac{a}{b}\left(\sum_{n=1}^{\infty}(A_{0n})_{\mathrm{L}}(n\pi)\sin(n\pi Y) + \sum_{m-1}^{\infty} \times \sum_{n=1}^{\infty}(A_{mn})_{\mathrm{L}}(n\pi)\cos(m\pi X)\sin(n\pi Y)\right) \quad (12b)$$

However, as $(A_{0n})_{\mathrm{L}} = (A_{mn})_{\mathrm{L}} = 0$, this implies that $V(x,y)_{\mathrm{L}} = 0$. Therefore, the liquid flow in the wick structure is only one-dimensional when this line heater is positioned along the heat pipe width from $0 \le y \le b$.

2.2. Strip heater

The liquid flow solutions for the strip heating condition can also be evaluated using similar approach. Consider a strip heater that lies between $x_i \le x \le x_j$ and $0 \le y \le b$ on the heat pipe as illustrated in Fig. 2(c) where the source distribution function is described as follows,

$$f(x,y)_S = \begin{cases} 1, & x < x_i,\ x > x_j \\ -\eta_S, & x_i \le x \le x_j \end{cases} \tag{13}$$

The liquid pressure solution per unit strength in the wick structure for the strip heater can be evaluated as:

$$\begin{aligned} P(x,y)_S &= \left(\frac{1}{-\eta_P}\right) \iint_R f(x,y)_S G(x,y|x_1,y_1) dx_1 dy_1 \\ &= \sum_{m=1}^{\infty} (A_{m0})_S \cos(m\pi X) + \sum_{n=1}^{\infty} (A_{0n})_S \cos(m\pi Y) + \sum_{m-1}^{\infty} \\ &\quad \times \sum_{n=1}^{\infty} (A_{mn})_S \cos(m\pi X) \cos(n\pi Y) \end{aligned} \tag{14}$$

where the Fourier coefficients $(A_{m0})_S$, $(A_{0n})_S$ and $(A_{mn})_S$ are evaluated to be:

$$(A_{m0})_S = -(1+\eta_S)\left(\frac{2a}{b(m\pi)^3}\right)\left[\sin\frac{m\pi x_j}{a} - \sin\frac{m\pi x_i}{a}\right] \tag{15a}$$

$$(A_{0n})_S = 0 \tag{15b}$$

$$(A_{mn})_S = 0 \tag{15c}$$

The dimensional rate ratio of η for the strip heater is formulated by considering the mass conservation along with the heat pipe dimensions. Hence, it is determined to be:

$$\eta_S = \frac{a}{(x_j - x_i)} - 1 \tag{16}$$

Since $(A_{0n})_S = (A_{mn})_S = 0$, as a result, the liquid flow $U(x,y)_S$ will still be a one-dimensional flow in the x-direction since $V(x,y)_S = 0$. Thus, the $U(x,y)_S$ solution per unit strength can be expressed as follows:

$$U(x,y)_S = \sum_{m=1}^{\infty} (A_{m0})_S (m\pi) \sin(m\pi X) \tag{17}$$

2.3. Discrete heater

Similar approach could also be adopted to determine the liquid flow solutions for the discrete heating condition. For illustration, consider a discrete heater with the following dimensions, $x_i \le x \le x_j$ and $y_i \le y \le y_j$ on the flat plate heat pipe as shown in Fig. 2(d). The source distribution function of this heating condition is represented below:

$$f(x,y)_D = \begin{cases} 1, & 0 \le x \le x_i,\ 0 \le x \le b \\ 1, & x_j \le x \le a;\ 0 \le x \le b \\ -\eta_D, & x_i \le x \le x_j,\ y_i \le y \le y_j \\ 1, & x_i \le x \le x_j,\ 0 \le y \le y_i \\ 1, & x_i \le x \le x_j,\ y_j \le y \le b \end{cases} \tag{18}$$

Hence, using the Green's function application, the liquid pressure solution per unit strength for the discrete heating condition can be simplified to be:

$$\begin{aligned} P(x,y)_D &= \left(\frac{1}{-\eta_P}\right) \iint_R f(x,y)_D G(x,y|x_1,y_1) dx_1 dy_1 \\ &= \sum_{m=1}^{\infty} (A_{m0})_D \cos(m\pi X) + \sum_{n=1}^{\infty} (A_{0n})_D \cos(m\pi Y) + \sum_{m-1}^{\infty} \\ &\quad \times \sum_{n=1}^{\infty} (A_{mn})_D \cos(m\pi X) \cos(n\pi Y) \end{aligned} \tag{19}$$

where the Fourier coefficients $(A_{m0})_D$, $(A_{0n})_D$ and $(A_{mn})_D$ are found to be:

$$(A_{m0})_D = -(1+\eta_D)\left(\frac{2a}{b^2(m\pi)^3}\right)\left(y_j - y_i\right)\left[\sin\frac{m\pi x_j}{a} - \sin\frac{m\pi x_i}{a}\right] \tag{20a}$$

$$(A_{0n})_D = -(1+\eta_D)\left(\frac{2b}{a^2(n\pi)^3}\right)(x_j - x_i)\left[\sin\frac{n\pi y_j}{b} - \sin\frac{n\pi y_i}{b}\right] \tag{20b}$$

$$\begin{aligned} (A_{mn})_D = -(1+\eta_D)\left(\frac{4ab}{nb^2m^3\pi^4 + ma^2n^3\pi^4}\right)\left[\sin\frac{m\pi x_j}{a}\right. \\ \left. - \sin\frac{m\pi x_i}{a}\right]\left[\sin\frac{n\pi y_j}{b} - \sin\frac{n\pi y_i}{b}\right] \end{aligned} \tag{20c}$$

Similarly, the dimensional rate ratio η_D of this discrete heating condition can be reduced after considering the mass conservation, where,

$$\eta_D = \frac{ab}{(x_j - x_i)\left(y_j - y_i\right)} - 1 \tag{21}$$

Moreover, the liquid flow is two-dimensional and the expressions of the corresponding velocity components in this discrete heating condition are determined to be:

$$\begin{aligned} U(x,y)_D &= \sum_{m=1}^{\infty} (A_{m0})_D (m\pi) \sin(m\pi X) + \sum_{m-1}^{\infty} \\ &\quad \times \sum_{n=1}^{\infty} (A_{mn})_D (m\pi) \sin(m\pi X) \cos(n\pi Y) \end{aligned} \tag{22a}$$

$$\begin{aligned} V(x,y)_D = \frac{a}{b}\Bigg\{ &\sum_{n=1}^{\infty} (A_{0n})_D (n\pi) \sin(n\pi Y) + \sum_{m-1}^{\infty} \\ &\times \sum_{n=1}^{\infty} (A_{mn})_D (n\pi) \cos(m\pi X) \sin(n\pi Y) \Bigg\} \end{aligned} \tag{22b}$$

Hence, by employing the Green's function approach with the respective source distribution functions, it is possible to study the liquid flow performances when there are multiple discrete heaters on the heat pipe.

3. Results and discussion

Following the method employed by Tan et al. [5], the infinite series used in the analytical solutions are truncated at $m = n = 40$ where further increment in the Fourier terms will have no significant improvement to the final results. The liquid pressure fields to be shown are the pressure drop contours with non-dimensional pressure difference of $\Delta P(X,Y) = (P - P_{\min})$ where $P_{\min}$ is the non-dimensional minimum pressure in the wick structure of the heat pipe. As for the liquid velocity contours in the wick structure, the velocity fields are represented with vectors in the form of, $\overrightarrow{V} = U_i + V_j$.

The results of the liquid pressure and velocity distributions are demonstrated for the conditions when there are line, strip and discrete heating conditions being simulated on the heat pipe respectively.

3.1. Line heater

The liquid pressure and the velocity distributions are determined when a line heater is positioned along the x-direction where $x_1/a = 0.5$ on the heat pipe. In Fig. 3(a), it illustrates the liquid pressure drop contours from the effects of this line heater inside the heat pipe. The resulting maximum liquid pressure difference across the wick structure is found to be $\Delta P_{\max} = 0.124$. As the shown in Fig. 3(b), the liquid flow is one-dimensional and it is observed that the liquid returns to the common line location from the two extreme ends of the heat pipe.

Fig. 4(a) and (b) show another illustration of the liquid pressure and velocity distributions when there are two line heaters with equal heat input strength on the heat pipe. Consider these two line heaters which are perpendicular to each other and they are positioned along the $x_1/a = 0.5$ and $y_1/b = 0.5$ axes respectively. These two lines will meet at a common point, which is at the center of the heat pipe. In this heating condition, the maximum

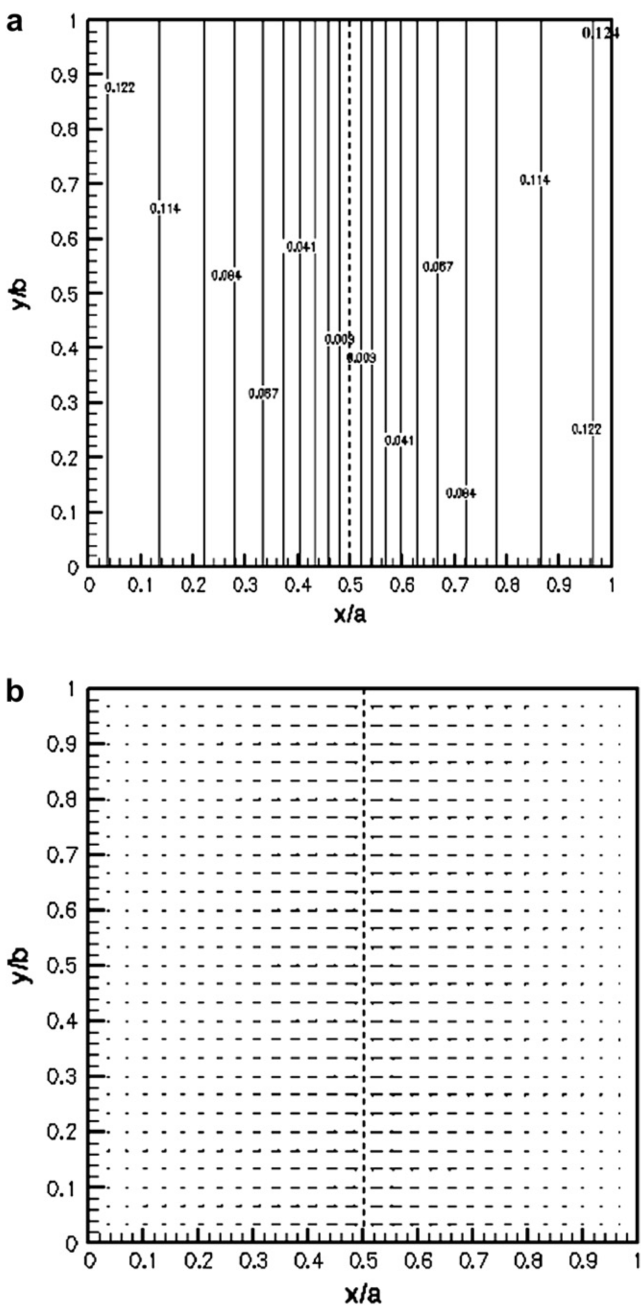

Fig. 3. Pressure (a) and velocity (b) distributions of a line heater at $x_1/a = 0.5$ axis on the flat plate heat pipe (*Dotted line represents the line heater*).

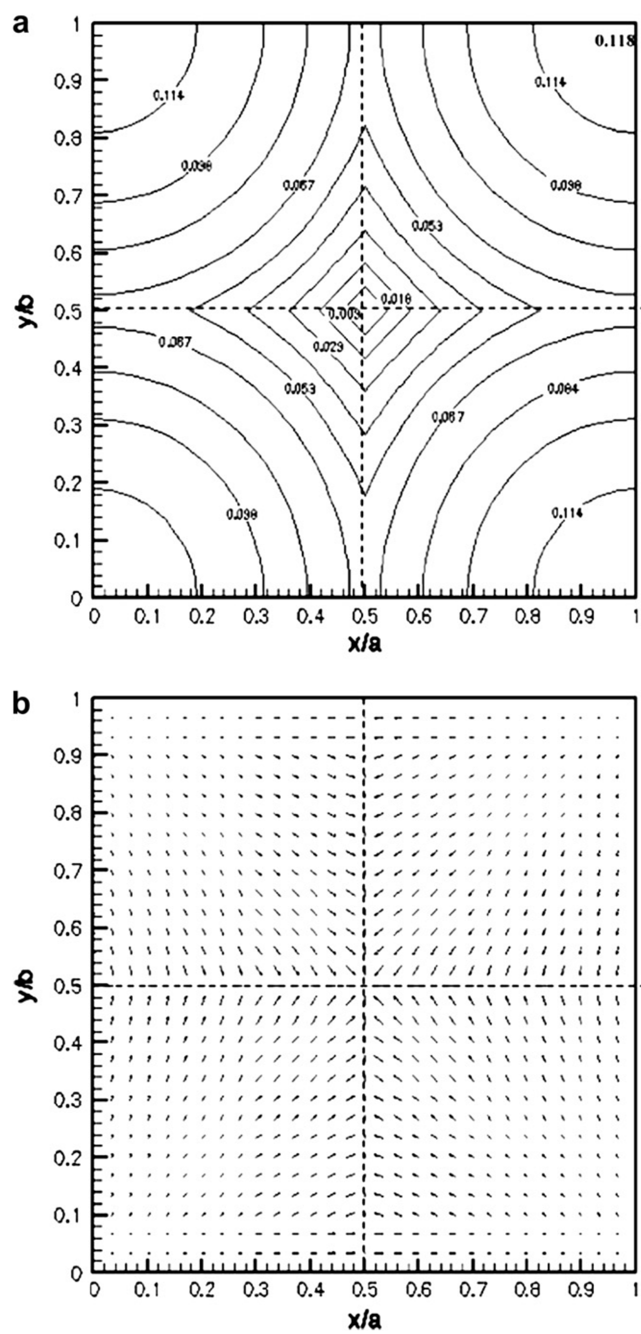

Fig. 4. Pressure (a) and velocity (b) distributions of 2 line heaters at $x_1/a = 0.5$ and $y_1/b = 0.5$ axes respectively on the flat plate heat pipe (*Dotted line represents the line heater*).

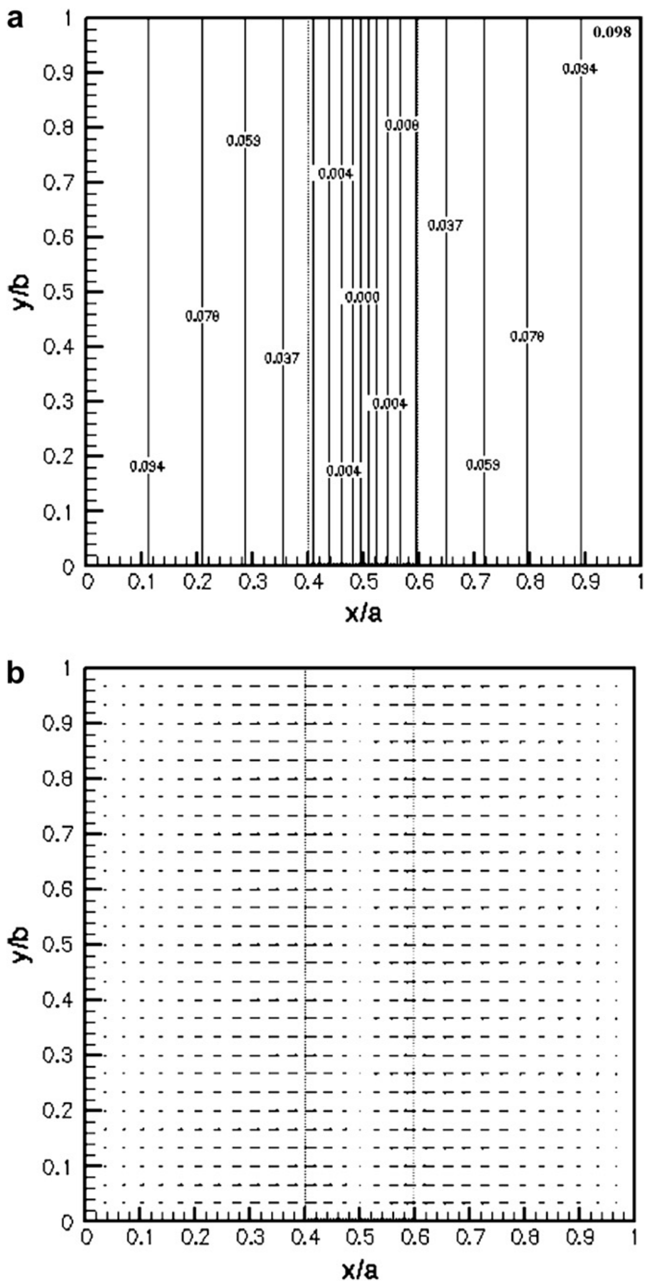

Fig. 5. Pressure (a) and velocity (b) distributions of a strip heater with dimension $0.4 \le x/a \le 0.6$, $0 \le y/b \le 1$ on the flat plate heat pipe.

liquid pressure drop $\Delta P_{\max}$ is slightly lower at about 0.118 as shown in Fig. 4(a). And similarly, with one more line heating condition on the heat pipe, the liquid will have more return paths to the heat source positions after condensation. Hence, the maximum liquid pressure will be lower as the returning path for the liquid will be shorter as compared to the illustration shown in Fig. 3(a).

The liquid flow is two-dimensional as shown in Fig. 4(b). This could be attributed to the overlapping point of these two line heaters. It is observed that at regions nearer to the center of the heat pipe, the liquid is being directed towards the center of the heat pipe, which is the overlapping point of these two line heaters. At this overlapping point, the heat flux is doubled and therefore the liquid will tend to return to this position. At regions that are further

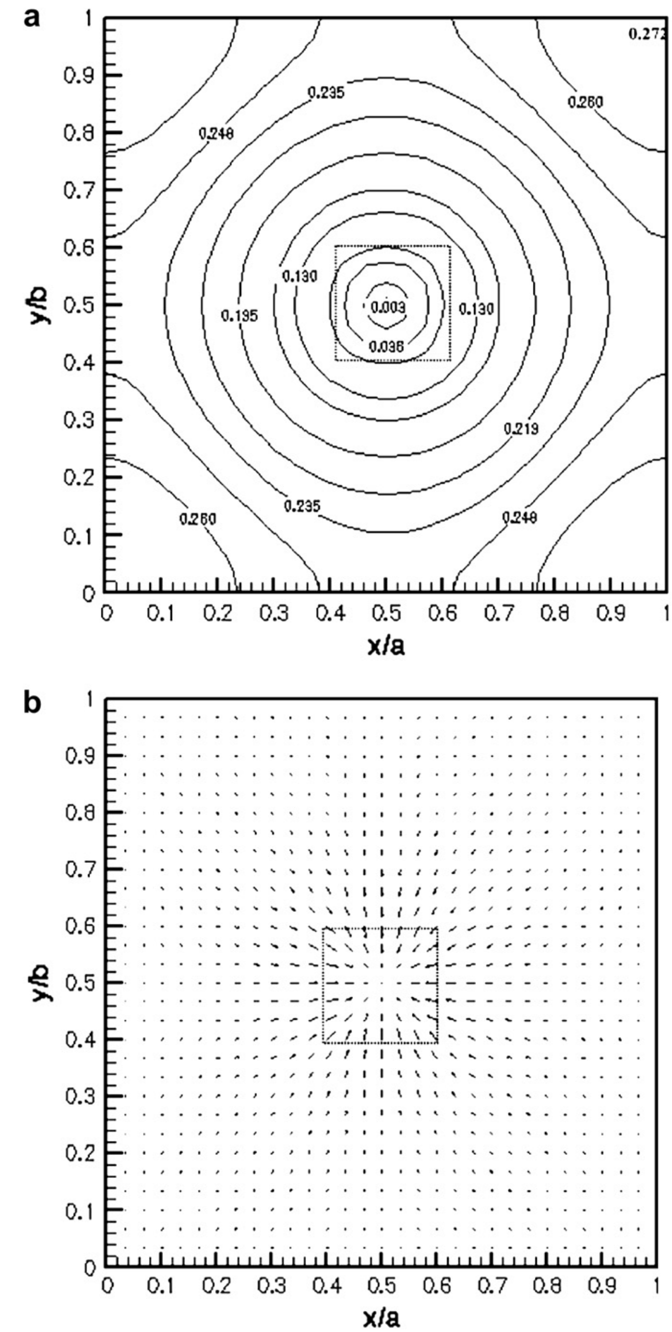

Fig. 6. Pressure (a) and velocity (b) distributions of a discrete heater at its optimum position of $x_c/a = y_c/b = 0.5$.

away from this overlapping point, the liquid is observed to be heading towards the ends of the line heaters.

3.2. Strip heater

Consider a strip heating condition with its normalized dimensions being defined to be $0.4 \le x/a \le 0.6$ and $0 \le y/b \le 1$ on the heat pipe where $x_i/a = 0.4$ and $x_j/a = 0.6$. From Fig. 5(a), it shows the liquid pressure contours that are similar to the line heating condition as demonstrated in Fig. 3(a). It is observed that the maximum liquid pressure, $\Delta P_{\max}$ is much lower at a value of 0.098. This could be attributed to the presence of a larger heater

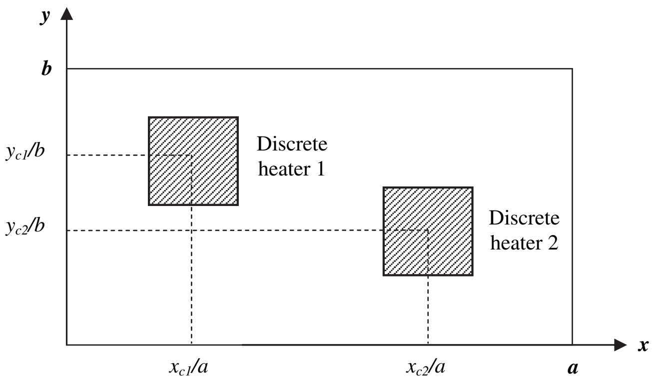

Fig. 7. Geometrical definition of two arbitrarily positioned discrete heaters on the flat plate heat pipe.

surface and therefore the liquid's return path to the strip heater is substantially shorter.

The flow is also one-dimensional for the liquid inside the wick structure as shown in Fig. 5(b). In addition, it is observed that the returning liquid is directed towards the center of the strip heater before the vaporization of the working fluid starts again inside the heat pipe.

3.3. Discrete heater

The discrete heating condition on the heat pipe is also simulated using the Green's function approach. This is made possible by considering the necessary heater boundary conditions during the analysis. It is always advantageous to model the heat sources as discrete heaters, as it will closely represent the actual IC chip dimensions on a PCB.

For illustration, consider a discrete heater with the normalized dimensions of $x_j - x_i/a = y_j - y_i/b = 0.2$ which is modeled to simulate a typical IC chip. In this simulation, the normalized center coordinates of this discrete heater are also defined for the positioning requirement for the discrete heater on the heat pipe, such that: $x_c/a = x_j - x_i/2b; y_c/b = y_j - y_i/2b$.

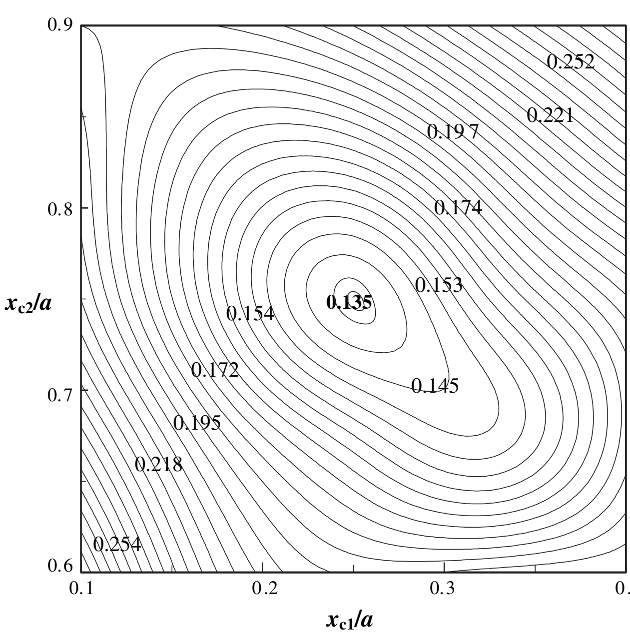

Fig. 8. The maximum liquid pressure drop contours of various discrete heater arrangements with different x_{c1}/a and x_{c2}/a values.

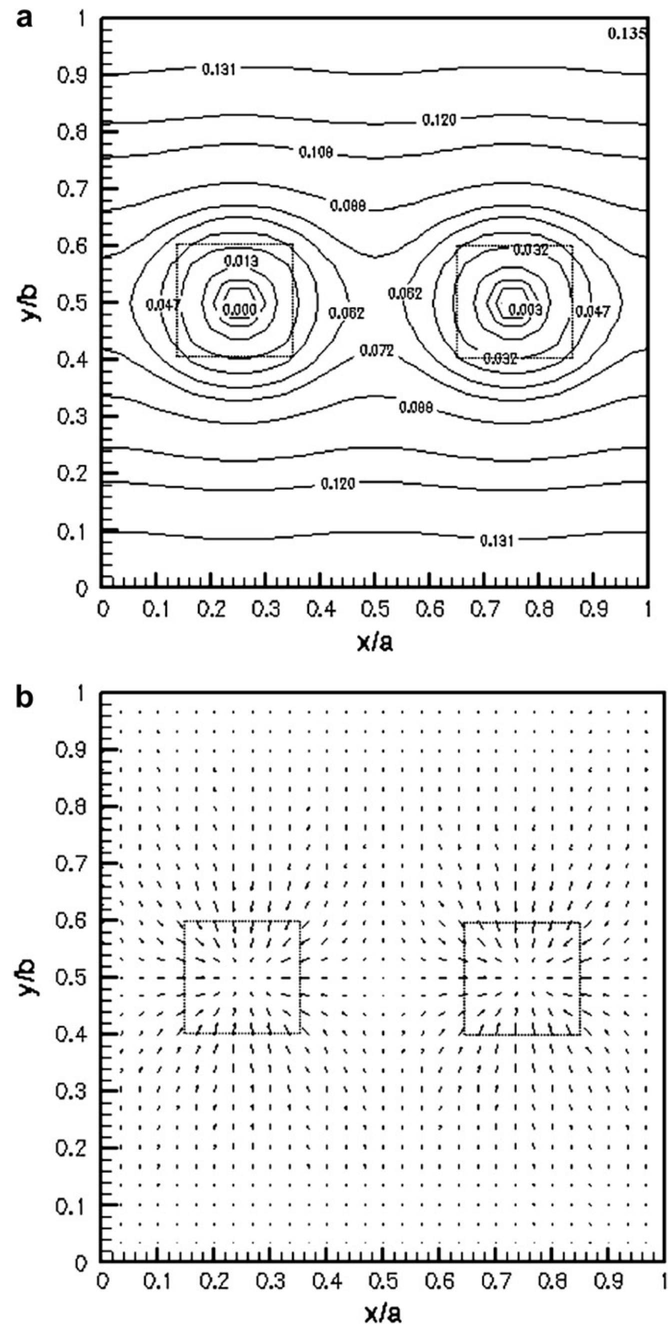

Fig. 9. Pressure (a) and velocity (b) distributions of two discrete heaters at their optimum position of $x_{c1}/a = 0.25$ and $x_{c2}/a = 0.75$.

Fig. 6(a) and (b) clearly illustrate the liquid flow performances under this discrete heating condition at the center of the heat pipe where $x_c/a = y_c/b = 0.5$. From the liquid pressure drop contours in Fig. 6(a), the maximum liquid pressure drop ΔP_{max} is found to be at about 0.272. As shown in Fig. 6(b), the flow is two-dimensional and it is observed that the liquid is directed towards the center of the discrete heater from all directions inside the heat pipe.

The Green's function approach is then extended to model with two discrete heaters on the heat pipe. This work is most appropriate, as it simulates multiple IC chips heating condition on the heat pipe. For demonstration, consider two discrete heaters with

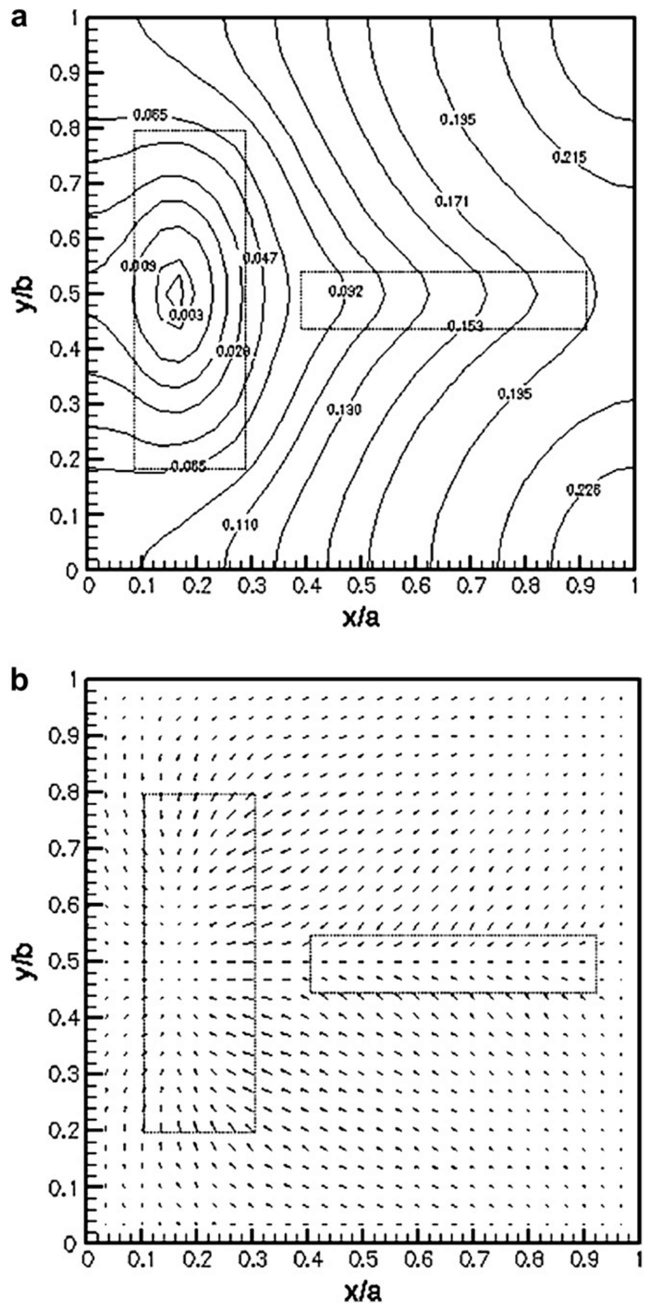

Fig. 10. Pressure (a) and velocity (b) distributions of two discrete heaters with different dimensions.

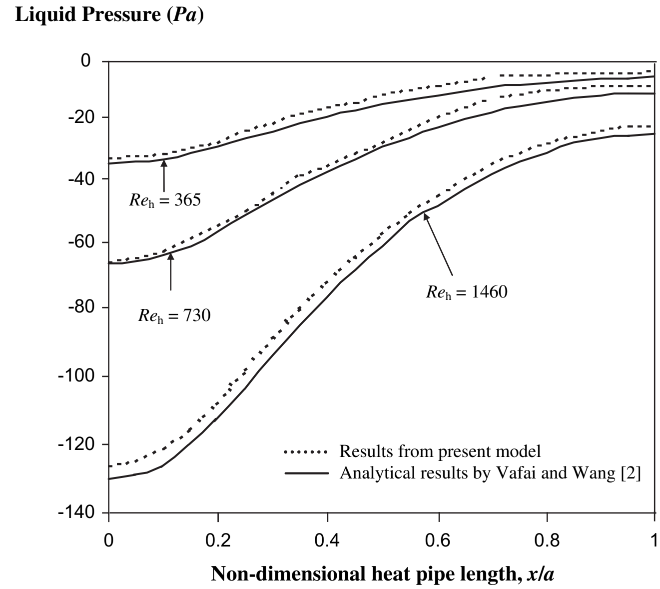

Fig. 11. Comparison of the liquid pressure results using the present model with the analytical solutions given in the literature.

the same dimensions as the single discrete heater described in Fig. 6(a) and (b). In addition, to facilitate the positioning requirement of these heaters, the respective heater center positions of (x_{c1}/a, y_{c1}/b) and (x_{c2}/a, y_{c2}/b) are defined as shown in Fig. 7.

Optimum heater positions are also determined for these two discrete heaters with the same heat input strength on the heat pipe. For illustration, consider these heaters that vary along the same $y_{c1}/b = y_{c2}/b = 0.5$ axis on the heat pipe, the optimum positions are found when the two heaters are at $x_{c1}/a = 0.25$ and $x_{c2}/a = 0.75$ respectively. This optimum heater arrangement is found when the corresponding maximum liquid pressure drop ΔP_{max} is the lowest. As shown in Fig. 8, it illustrates the maximum liquid pressure drop contours of the various heater arrangements with different x_{c1}/a and x_{c2}/a values along the same $y_{c1}/b = y_{c2}/b = 0.5$ axis on the heat pipe. The optimum arrangement is determined when ΔP_{max} of 0.135 is the least as compared to the other heater arrangements. The liquid pressure and velocity distributions for this optimum heater arrangement are shown in Fig. 9(a) and (b) where symmetrical pressure drop contours as well as identical flow patterns are observed respectively.

Besides simulating the discrete heaters of identical dimensions, it is also possible to simulate heaters with different dimensions on the heat pipe. This simulation is realistic, as it will represent the different IC chip dimensions on the heat pipe. Fig. 10(a) and (b) show the liquid pressure drop and velocity distributions of a typical illustration when there are two discrete heaters of different dimensions on the heat pipe. Under this kind of heating condition, the liquid flow performance is dependent on the size and position of the heaters on the heat pipe. The optimum heater positions can be determined and the results will be beneficial where the maximum heat pipe performance can be achieved when these heaters are optimally positioned. Hence, by using the Green's function approach, heaters of different types and dimensions can be modeled which will provide realistic simulation of the IC chips on the heat pipe.

3.4. Validation of the analytical model

The analytical liquid flow model presented in this paper is validated with another analytical model developed by Vafai and Wang [2]. The work presented by Vafai has employed an integral analysis method to investigate the flow performances inside a flat plate heat pipe. Their analytical work has provided a more complete representation as the vapor and liquid flow inside the heat pipe were considered in their integral approach. Hence, the model is used as the basis to validate with the present liquid flow methodology.

A strip heating condition was considered in Vafai's model to evaluate the vapor and liquid pressure performances across the heat pipe. The conditions and parameters used in the model were then incorporated into the present liquid flow model, which uses the Green's function analysis to simulate the strip heating effects on the heat pipe (heater region is at $0 \le x/a \le 0.2$). The liquid pressure results were obtained for the various flow conditions with different injection Reynolds number, Re_h, where h is the vapor space height of the heat pipe.

Fig. 11 clearly shows the comparison of the liquid pressure distributions between the present model and the analytical solutions presented by Vafai. Relatively similar pressure distribution trends were observed at each Re_h numbers, starting from the heat source region to the entire heat pipe length. Since there is a relative good agreement between the two models, hence it is deduced that the present liquid flow model is appropriate to evaluate the liquid flow performances in the wick structure of a flat plate heat pipe.

3.5. Usefulness of the analytical model

It is possible to employ the model to determine the optimum heaters' location on a flat plate heat pipe via the knowledge of the analytical ΔP_{max} values. At different heaters' locations, different ΔP_{max} values could be obtained analytically and these will correspond to the different liquid temperatures on a flat plate heat pipe. The optimum heaters' location could then be determined when the minimum ΔP_{max} value is identified. This will therefore correspond to the lowest surface temperature achieved. In application, the discrete heating conditions could be modeled as a realistic simulation of IC chips. This enables the electronic system designer to obtain the optimum IC chip positions on a PCB. Hence the heat dissipation will be optimum whilst the IC chips are maximally cooled using a flat plate heat pipe.

4. Concluding remarks

The analytical liquid flow model presented in this paper using the Green's function approach is capable of predicting qualitatively the pressure and velocity distributions under the conditions with different types of heat sources on a flat plate heat pipe. The results with line, strip and discrete heating conditions on the heat pipe were presented. Moreover, multiple heat source conditions on the heat pipe were also simulated. More importantly, the analytical liquid flow model is validated with the results obtained in the literature. With the comparable results, the liquid flow model is competent to predict the liquid flow distribution in the wick structure of the heat pipe under different heating conditions. In application, by simulating discrete heating conditions as the IC chips' heating configuration, this analytical model is applicable and useful to determine optimum IC chip positions on a PCB. This will enable designer to better position the IC chips optimally in their electronic system design.

References

[1] A. Faghri, Heat Pipe Science and Technology, Taylor and Francis, Washington D.C., 1995.
[2] K. Vafai, B. Wang, Analysis of flow and heat transfer characteristics of an asymmetrical flat plate heat pipe, International Journal of Heat and Mass Transfer 35 (1992) 2087–2099.
[3] X.Y. Huang, C.Y. Liu, The pressure and velocity fields in the wick structure of a localized heated flat plate heat pipe, International Journal of Heat and Mass Transfer 39 (1996) 1325–1330.
[4] A. Faghri, M. Buchko, Experimental and numerical analysis of low temperature heat pipes with multiple heat sources, ASME Journal of Heat Transfer 113 (1991) 728–734.
[5] B.K. Tan, X.Y. Huang, T.N. Wong, K.T. Ooi, A study of multiple heat sources on a flat plate heat pipe using a point source approach, International Journal of Heat and Mass Transfer 43 (2000) 3755–3764.
[6] G. Stephenson, Partial Differential Equations for Scientists and Engineers, third ed. Longman Inc., New York, 1985.